

Hydrodynamic Lyapunov modes and strong stochasticity threshold in Fermi-Pasta-Ulam models

Hong-liu Yang* and Günter Radons†

Institute of Physics, Chemnitz University of Technology, D-09107 Chemnitz, Germany

(Received 7 December 2005; published 1 June 2006)

The existence of a strong stochasticity threshold (SST) has been detected in many Hamiltonian lattice systems, including the Fermi-Pasta-Ulam (FPU) model, which is characterized by a crossover of the system dynamics from weak to strong chaos with increasing energy density ϵ . Correspondingly, the relaxation time to energy equipartition and the largest Lyapunov exponent exhibit different scaling behavior in the regimes below and beyond the threshold value. In this paper, we attempt to go one step further in this direction to explore further changes in the energy density dependence of other Lyapunov exponents and of hydrodynamic Lyapunov modes (HLMs). In particular, we find that for the FPU- β and FPU- $\alpha\beta$ models the scalings of the energy density dependence of all Lyapunov exponents experience a similar change at the SST as that of the largest Lyapunov exponent. In addition, the threshold values of the crossover of all Lyapunov exponents are nearly identical. These facts lend support to the point of view that the crossover in the system dynamics at the SST manifests a global change in the geometric structure of phase space. They also partially answer the question of why the simple assumption that the ambient manifold representing the system dynamics is quasi-isotropic works quite well in the analytical calculation of the largest Lyapunov exponent. Furthermore, the FPU- β model is used as an example to show that HLMs exist in Hamiltonian lattice models with continuous symmetries. Some measures are defined to indicate the significance of HLMs. Numerical simulations demonstrate that there is a smooth transition in the energy density dependence of these variables corresponding to the crossover in Lyapunov exponents at the SST. In particular, our numerical results indicate that strong chaos is essential for the appearance of HLMs and those modes become more significant with increasing degree of chaoticity.

DOI: [10.1103/PhysRevE.73.066201](https://doi.org/10.1103/PhysRevE.73.066201)

PACS number(s): 05.45.Jn, 05.20.-y, 05.45.Pq, 05.45.Xt

I. INTRODUCTION

In spite of the great success in predicting properties of systems from their microscopic details, some fundamental issues at the basis of statistical mechanics are still under discussion [1–6]. One important example is the validity of the ergodicity hypothesis. This partially explains the continuous and growing research interest in the nonlinear dynamics of high-dimensional Hamiltonian systems during the last decades.

Based on a theorem by Poincaré and Fermi [7], which states that under general perturbations the total energy is the only possible integral invariant in a Hamiltonian system with $N \geq 3$ degrees of freedom, a Hamiltonian system with a large number of degrees of freedom is expected to be ergodic and its long-time behavior should follow the predictions of statistical mechanics. In this context, the result reported in the celebrated work by Fermi, Pasta, and Ulam (FPU) in 1955 came as a surprise [8]. They attempted to use numerical experiments to check whether a high-dimensional Hamiltonian system starting from nonequilibrium initial conditions would relax to equilibrium eventually. Instead of the anticipated energy equipartition among all normal modes, they saw a recurrent flow of energy among modes in a lattice of oscillators with anharmonic couplings. This challenges greatly the validity of statistical mechanics in high-dimensional nonintegrable Hamiltonian systems. It seemed that the difficulty

could be resolved, at least partially, by applying the contemporary Kolmogorov-Arnold-Moser (KAM) theory [9], which states that a positive measure of invariant tori persist if the perturbation remains below a certain threshold. Subsequently improved estimates showed, however, that the threshold value decreases exponentially with increasing number of degrees of freedom [10,11]. Therefore the persistence of KAM tori should not be an obstacle to the approach to energy equipartition in FPU's experiment. On the other hand, some authors claimed that a threshold of stochasticity or equipartition is detected in their numerical experiments with various model systems including the FPU model and the Lennard-Jones chain [12–14]. Moreover, there have been numerical simulations which indicate the persistence of the threshold in the thermodynamic limit [14]. Further careful numerical work carried out in the last two decades clarified that such a threshold does not characterize a transition from regular to chaotic states [15,16]. Instead, it corresponds to a smooth transition in the system dynamics between weak and strong chaos. In other words, the equipartition of energy can almost always be achieved in these high-dimensional nonlinear Hamiltonian systems [17] and the only matter of concern is the duration of the relaxation time to such a state [15,16]. Therefore, the smooth transition in the chaoticity of the system dynamics is called the strong stochasticity threshold (SST)[16]. In the low-energy regime below the SST, the relaxation time to energy equipartition grows as a stretched exponential law of the energy density. Beyond the transition the relaxation time is almost independent of the energy density. Besides, a remarkable change in the scaling laws of the largest Lyapunov exponent also takes place at SST. Up to now, similar results have been reported for a large number of

*Electronic address: hongliu.yang@physik.tu-chemnitz.de†Electronic address: radons@physik.tu-chemnitz.de

systems [18–21], which indicates that the existence of the SST is a quite general aspect of Hamiltonian systems with many degrees of freedom.

In a series of recent papers [22–26] Pettini and co-workers developed further the geometry theory of Hamiltonian chaos pioneered by Krylov [1]. The nonperturbative nature of this approach facilitates the study of the origin of Hamiltonian chaos and the SST in high-dimensional Hamiltonian systems. They provided evidence that the transition in the system dynamics at the SST manifests a certain dramatic change in the geometric structure of configuration space [22,23]. The existence of a direct relation between the curvature properties of the ambient manifold representing the system dynamics and the Lyapunov instabilities of system trajectories encourages an understanding of the physical origin of the SST from the point of view of nonlinear dynamics.

Since the transition at the SST is anticipated as a global change in the geometric structure of phase space, and results of previous investigations are in favor of such a statement [22,23], we expect that there should be changes in other indicators of the instability of trajectories, not only in the largest Lyapunov exponent. The aim of the current paper is to explore the possible changes in the whole Lyapunov spectrum and in the so-called hydrodynamic Lyapunov modes (HLMs) [27] in connection with the SST.

Hydrodynamic Lyapunov modes are wavelike structures in Lyapunov vectors associated with near-zero Lyapunov exponents of high-dimensional dynamical systems. Their existence was first reported in many-particle systems with hard-core interactions by Posch and co-workers [27]. This discovery immediately triggered great interest of many research groups due to its potential importance for an understanding of the fundamental problems of statistical mechanics from the point of view of nonlinear dynamics [28–38]. The existence of HLMs has already been reported for various systems ranging from many-particle systems with hard-core [28,32] or soft-potential interaction [34–36], products of random matrices [29], and coupled map lattices [37] to the Kuramoto-Shivashinsky equation [38]. Although a lot of work has already been carried out both numerically and analytically [28–38], a thorough understanding of this subject has not yet been achieved. A common belief is that continuous symmetries and conservation laws are essential for the appearance of HLMs, which is also supported by previous studies. In the current paper we try to show for Hamiltonian lattice models that strong chaos is also important for the appearance of such modes. In particular, the FPU- β model is selected as an example to illustrate that HLMs exist in Hamiltonian lattice models with continuous symmetries. Some indicators are defined to measure the significance of HLMs. The dependence of these indicators on the energy density is investigated in detail. Numerical simulations demonstrate that these quantities show quite different behavior in the regimes of weak and strong chaos, respectively.

The remainder of the paper is organized as follows. The model systems under investigation and the details of the numerical simulations are given in Sec. II. In order to facilitate the reading of this paper, we will recall briefly in Sec. III the correlation function theory of Lyapunov vectors. In Sec. IV the results of numerical simulations with respect to the

changes in the Lyapunov spectrum and in HLMs will be presented. Our focus here is on the FPU- β model while the case of the FPU- $\alpha\beta$ model is treated only briefly, since the scenarios in the two systems are quite similar. We will study in Sec. V how a change in the system size influences the results presented in the previous sections and clarify the role played by the fluctuations of finite-time Lyapunov exponents. Finally we will summarize the main results and end the paper with a short discussion.

II. MODELS

Two cases of the one-dimensional FPU model are used to demonstrate the changes in Lyapunov spectrum and in hydrodynamic Lyapunov modes in connection with the crossover from weak to strong chaos. This class of models is described by a Hamiltonian of the form

$$H = \sum_{l=1}^L \left(\frac{p_l^2}{2} + V(q_{l+1} - q_l) \right) \quad (1)$$

where q_l denotes the displacement of the l th particle from its equilibrium position la , $p_l = \dot{q}_l$ is the conjugate momentum, and periodic boundary conditions $q_{L+1} = q_1$ are used. The potential $V(z)$ is of the form

$$V(z) = \frac{1}{2}z^2 + \frac{1}{3}\nu z^3 + \frac{1}{4}\mu z^4. \quad (2)$$

With different choices of the parameters μ and ν in Eq. (2) two variations of the FPU model can be defined, the so-called FPU- β model with $\mu \neq \nu = 0$ and the FPU- $\alpha\beta$ model with $\mu \neq 0$ and $\nu \neq 0$. Throughout the current study we set the parameter $\mu = 1.0$ for the FPU- β model and $\nu = 0.25$ and $\mu = \frac{2}{3}\nu$ for the FPU- $\alpha\beta$ model, respectively. The energy density $\epsilon \equiv E/L$, where E is the total energy, is used as a control parameter to investigate the variation in Lyapunov characteristics.

Note that the Hamiltonian Eq. (1) is invariant under the variable transformation $q'_l = q_l + c$ with an arbitrary constant c , since only internal forces among particles are present. As a consequence of the translational invariance, the total momentum $P \equiv \sum_{l=1}^L p_l$ is conserved in the models given above. The continuous symmetry and the corresponding conserved quantity are essential for the appearance of HLMs in those systems.

The equations of motion, which can be easily derived from the given Hamiltonian, are integrated with a fourth-order Runge-Kutta algorithm [39]. The so-called standard method invented by Benettin *et al.* and Shimada and Nagashima is adopted to calculate the Lyapunov exponents and Lyapunov vectors, which characterizes the local instabilities of the trajectories of the systems under investigation [40].

III. CORRELATION FUNCTIONS OF LYAPUNOV VECTORS

In a high-dimensional system the Lyapunov vectors associated with near-zero Lyapunov exponents are known to be spatially extended [41]. If, in addition, the system holds

some continuous symmetries, those Lyapunov vectors may exhibit certain wavelike coherent structures, namely, hydrodynamic Lyapunov modes [27]. In order to detect unambiguously the coherent structures in those Lyapunov vectors (LVs) and to characterize the hydrodynamic Lyapunov modes quantitatively, we have introduced the correlation function theory for Lyapunov vectors, which will be recalled briefly in this section. Details can be found in [34,35,37].

Following the definition of microscopic densities in molecular hydrodynamics [42], we introduce a dynamical variable called the *LV fluctuation density* as

$$\mathcal{U}^{(\alpha)}(r, t) = \sum_{l=1}^L \delta u_t^{(\alpha)l} \delta(r - r_l) \quad (3)$$

where r_l is the position coordinate of the l th element of the system under investigation and $\{\delta u_t^{(\alpha)l}\}$ is the coordinate part of the α th Lyapunov vector. Each Lyapunov vector of Hamiltonian systems has $2L$ entries, which reflects certain perturbations in the coordinate q_i and the momentum p_i of the particles. If we represent the α th Lyapunov vector as $(\delta q_t^{(\alpha)1}, \delta q_t^{(\alpha)2}, \dots, \delta q_t^{(\alpha)L}, \delta p_t^{(\alpha)1}, \delta p_t^{(\alpha)2}, \dots, \delta p_t^{(\alpha)L})$, then $\delta u_t^{(\alpha)l} = \delta q_t^{(\alpha)l}$. For the lattice models used here, the position coordinate is simply $r_l \equiv la$. We set the lattice constant $a=1$ throughout the remainder of this paper to simplify the calculations.

The spatial Fourier transformation of the LV fluctuation density reads

$$\mathcal{U}_k^{(\alpha)}(t) = \int \mathcal{U}^{(\alpha)}(r, t) e^{-ik \cdot r} dr = \sum_{l=1}^L \delta u_t^{(\alpha)l} e^{-ik \cdot r_l}. \quad (4)$$

The so-called static LV structure factor is defined as

$$S_u^{(\alpha\alpha)}(k) = \langle \mathcal{U}_k^{(\alpha)}(t) \mathcal{U}_{-k}^{(\alpha)}(t) \rangle, \quad (5)$$

where $\langle \dots \rangle$ represents the time average. As can be easily seen from Eq. (5), the static LV structure factor is nothing but the spatial Fourier spectrum of the LV fluctuation density $\mathcal{U}^{(\alpha)} \times(r, t)$. Therefore it is suited for the characterization of the spatial structure of Lyapunov vectors.

The dynamic LV structure factor is defined as

$$S_u^{(\alpha\alpha)}(k, \omega) = \int \langle \mathcal{U}_k^{(\alpha)}(t) \mathcal{U}_{-k}^{(\alpha)}(0) \rangle e^{i\omega t} dt, \quad (6)$$

which can provide detailed information on the dynamical behavior of Lyapunov vectors.

The success of these quantities in the detection and characterization of HLMs has been shown in our previous studies of Lennard-Jones fluids and coupled map lattices [34,35,37,38].

IV. NUMERICAL RESULTS FOR LYAPUNOV SPECTRA AND HYDRODYNAMIC LYAPUNOV MODES

In this section the model systems described in Sec. II will be used to illustrate the changes that are observed in the Lyapunov spectrum and the hydrodynamic Lyapunov modes as the energy density is increased.

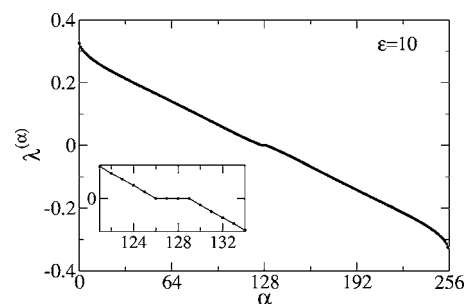


FIG. 1. Lyapunov spectrum of the FPU- β model with $\mu=1.0$ and $\epsilon=10$. Due to the Hamiltonian nature of the system the Lyapunov spectrum has the symmetry $\lambda^{(\alpha)} = -\lambda^{(2L-1-\alpha)}$. As can be seen from the inset, the system has four zero-value Lyapunov exponents. The system size used here is $L=128$.

A. FPU- β model

In this model the nature of the relaxation to energy equipartition has been extensively studied and the existence of the SST was first identified [14,16].

The Lyapunov spectrum for the case $\epsilon=10$ is shown in Fig. 1. Due to the Hamiltonian structure the spectrum has the symmetry $\lambda^{(\alpha)} = -\lambda^{(2L-1-\alpha)}$. As can be seen from the inset, the system has four zero-value Lyapunov exponents, which are related to the space and time translational invariance symmetries of the system and the associated conserved quantities, the total energy and the total momentum.

We present in Fig. 2 the change of the largest Lyapunov exponent $\lambda^{(1)}$ with increasing energy density ϵ . Note that the ascent of $\lambda^{(1)}$ with ϵ in the low-energy regime is much faster than in the high-energy regime. Numerical fitting of the ϵ dependence of $\lambda^{(1)}$ to a power law $\lambda^{(1)} \sim \epsilon^\beta$ yields $\beta \approx 2.0$ and 0.25 in the two regimes, respectively. A smooth transition connects the two different kinds of behavior at intermediate energy density values. As interpreted in previous studies [16], the change in the ϵ dependence of the largest Lyapunov exponent manifests a crossover of the system dynamics from weak to strong chaos. The critical energy density of the SST is roughly estimated as $\epsilon_c \approx 0.2$ for the current parameter setting.

Besides the above-mentioned change in the ϵ dependence of the largest Lyapunov exponent, we also expect to see changes in other indicators of the instability of trajectories,

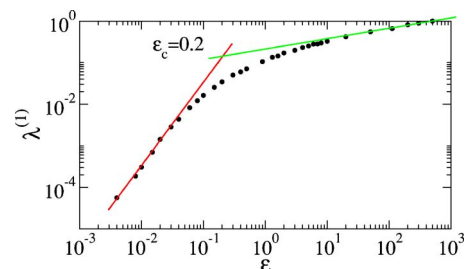


FIG. 2. (Color online) The largest Lyapunov exponent $\lambda^{(1)}$ vs energy density ϵ for the FPU- β model. The ϵ dependence of $\lambda^{(1)}$ is fitted to a power law with the exponents 2.0 and 0.25 in the low- and high-energy regimes, respectively. The threshold value of the crossover between the two regimes is $\epsilon_c \approx 0.2$.

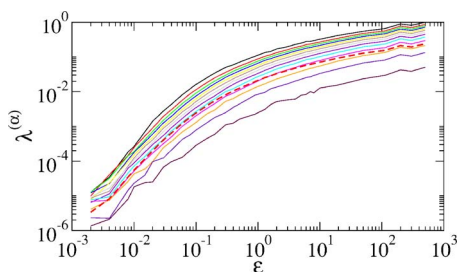


FIG. 3. (Color online) ϵ dependence of typical Lyapunov exponents in the positive branch of the Lyapunov spectrum for the FPU- β model. Here, α takes values from 1 to 121 with the increment 10 (from top to bottom). The density of the Kolmogorov-Sinai entropy $\rho_h \equiv h_{KS}/N$ is plotted as a dashed line. Obviously, all the Lyapunov exponents roughly follow the same trend as $\lambda^{(1)}$.

since the transition of the system dynamics at the SST is anticipated to be a global change in the geometric structure of phase space [16]. In Fig. 3 the ϵ dependence of other Lyapunov exponents sampled from the positive branch of the Lyapunov spectrum is presented. Obviously all of them follow the same tendency as the largest Lyapunov exponent, i.e., there are two scaling regimes at low and high energy densities, respectively, and they are mediated by a smooth transition in between.

The variation of the normalized Lyapunov exponents $\lambda^{(\alpha)}(\epsilon)/\lambda^{(\alpha)}(\epsilon_0)$ with the energy density is presented in Fig. 4. Roughly speaking all the data from different Lyapunov exponents collapse on a single curve. This demonstrates clearly that all Lyapunov exponents change in a similar way as the largest one. Moreover, the crossover in all Lyapunov exponents takes place at the same threshold value $\epsilon_c \approx 0.2$. On the one hand this result supports the above-mentioned point of view that there is a global change in the geometric structure of the phase space at the SST. On the other hand it explains why the strong assumption of quasi-isotropy works quite well in the analytical calculation of the largest Lyapunov exponent [24,25]. Under this assumption, the tensor equations governing the detailed dynamics of the local instabilities of the system trajectories are reduced to a simple scalar equation which describes the average instabilities of the given system. The form of the reduced equation does not depend on the detailed dynamics of the original system and only averaged properties of the curvatures of the ambient manifold enter as parameters. Roughly speaking, such an

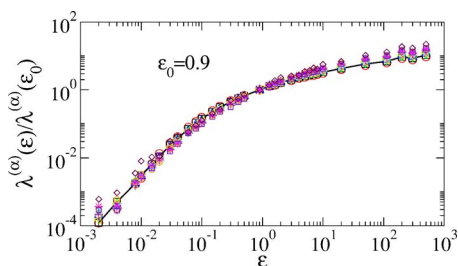


FIG. 4. (Color online) Normalized Lyapunov exponents $\lambda^{(\alpha)}(\epsilon)/\lambda^{(\alpha)}(\epsilon_0)$ vs energy density ϵ . Here the more or less arbitrary value $\epsilon_0=0.9$ was chosen. Note that all the data for different Lyapunov exponents collapse on one master curve.

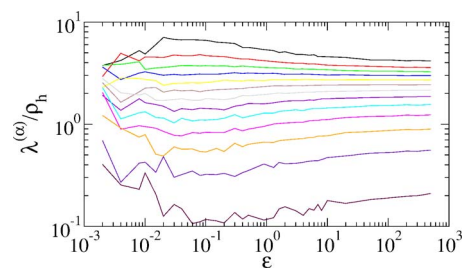


FIG. 5. (Color online) Lyapunov exponents normalized by the entropy density ρ_h vs energy density ϵ for the FPU- β model.

assumption implies that all the Lyapunov exponents of the system under investigation are identical. As Fig. 1 shows, this is not the case. An analytical estimate of the largest Lyapunov exponent based on this assumption, however, agrees with the numerical value quite well. Our results reported here provide an explanation for this puzzle. Although the values of the Lyapunov exponents differ from one another, they do have a similar ϵ dependence. In other words, apart from some constants, all the Lyapunov exponents contain the same information with respect to the tendency of change with ϵ . Therefore it comes as no surprise that one can obtain a correct estimate of the ϵ dependence of the largest Lyapunov exponent, or, of an effective measure of the average instability of the system dynamics, by using such a simple assumption.

As becomes obvious in Fig. 4 the collapse of the data is not perfect in the whole energy regime. To show this more clearly, we present in Fig. 5 the normalized Lyapunov exponents $\lambda^{(\alpha)}/\rho_h$, where $\rho_h = h_{KS}/L$ is the density of the Kolmogorov-Sinai entropy. These quantities are expected to be independent of ϵ , if all Lyapunov exponents have exactly identical ϵ dependence. The figure indicates that, apart from numerical errors, there are still deviations. In Sec. V we show that they can not be attributed to finite-size effects either. Therefore the occurrence of deviations from constants reflects the nature of the system dynamics.

We now turn to the characterization of Lyapunov vectors. The profiles of two prototypical Lyapunov vectors are shown in Fig. 6. The one associated with the largest Lyapunov ex-

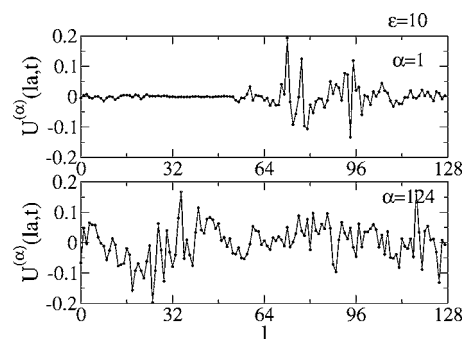


FIG. 6. Snapshots of two prototypical Lyapunov vectors for the FPU- β model with $\epsilon=10$. The Lyapunov spectrum is shown in Fig. 1. The LV (with $\alpha=1$) associated with the largest Lyapunov exponent is highly localized while the LV (with $\alpha=124$) corresponding to a near-zero Lyapunov exponent is spatially extended.

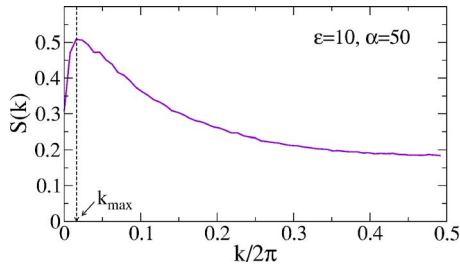


FIG. 7. (Color online) Static LV structure factor $S_u^{(\alpha\alpha)}(k)$ for a LV with $\alpha=50$. Here, k_{max} is defined as the wave number of the highest peak in the spectrum $S_u^{(\alpha\alpha)}(k)$.

ponent is highly localized in space. This aspect has been discussed for a long time [43–45] and a detailed study of the universal scenarios can be found in Ref. [45]. In contrast, the Lyapunov vector with $\alpha=124$, which is associated with a near-zero Lyapunov exponent, is spatially extended. Moreover, it exhibits a certain long-wavelength coherent structure, which indicates the existence of HLMs in this system.

For an accurate characterization of the spatial structure of the Lyapunov vectors, we adopt the measure of the static LV structure factor defined in Eq. (5). To simplify the notation, we will ignore the subscript and superscript of $S_u^{(\alpha\alpha)}(k)$ throughout the remainder of this paper. The static LV structure factor of an example case $\epsilon=10$ and $\alpha=50$ is presented in Fig. 7. It is characterized by the existence of a peak at k_{max} . Note that the associated Lyapunov exponent is already far from the center of the Lyapunov spectrum (see Fig. 1).

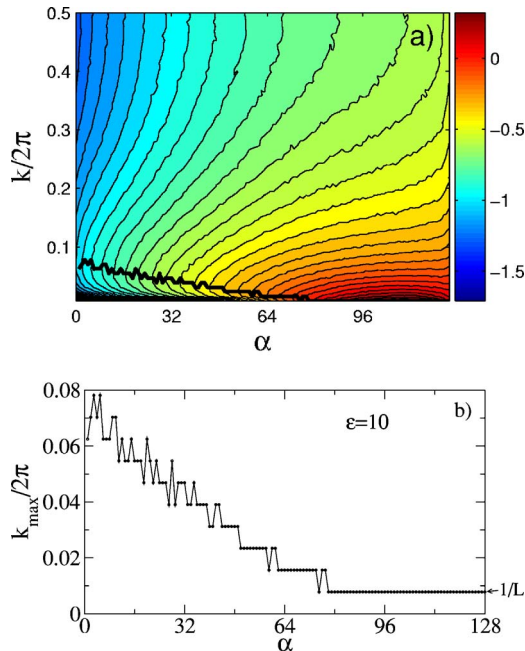


FIG. 8. (Color online) (a) Contour plot of static LV structure factors for the FPU- β model with $\epsilon=10$. (b) Variation of k_{max} with the index α of the LV. The Lyapunov vectors with $\alpha \approx 128$ are dominated by components with small wave numbers comparable to $2\pi/L$, which is the smallest nontrivial wave number permitted by the periodic boundary conditions used. These facts together imply the existence of hydrodynamic Lyapunov modes in this system.

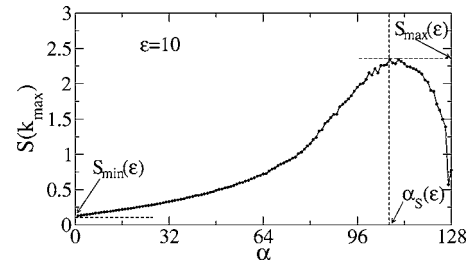


FIG. 9. $S(k_{max})$ vs α for the FPU- β model with $\epsilon=10$. $S_{max}(\epsilon)$, $S_{min}(\epsilon)$, and $\alpha_S(\epsilon)$ are defined to measure the significance of HLMs.

Therefore, the peak in the static LV structure factor is not so sharp.

The contour plot of the static LV structure factors for the whole set of Lyapunov vectors is shown in Fig. 8. It is obvious that the static LV structure factors of Lyapunov vectors associated with near-zero Lyapunov exponents are strongly dominated by certain components with low wave numbers. As shown in Fig. 8(b), the wave number k_{max} of the dominant peak approaches $2\pi/L$ gradually as the index α of Lyapunov vectors goes to 128, i.e., as the associated Lyapunov exponents approach zero. The variation of $S(k_{max})$ and the spectral entropy H_S as function of the index α are presented in Figs. 9 and 10, respectively, where $S(k_{max})$ denotes the height of the dominant peak of the static structure factor of a given Lyapunov vector and the spectral entropy H_S is defined as $H_S \equiv -\sum S(k) \ln S(k)$. A smaller value of H_S and a larger value of $S(k_{max})$ indicate the existence of a sharp peak in the static LV structure factor under investigation. Numerical data show that both quantities attain their extreme values at $\alpha \approx 108$. Combined with the fact that the wave numbers k_{max} of the dominant peaks are near to $2\pi/L$ in this regime, these numerical results demonstrate the existence of HLMs in this system.

To illustrate the changes in the Lyapunov vectors with increasing energy density, the variations of the quantities $S(k_{max})$, k_{max} and H_S are shown in Fig. 11 for several Lyapunov vectors with the associated Lyapunov exponents in the positive branch of the Lyapunov spectrum. All three variables exhibit qualitatively different behavior in the low- and high-energy regimes. Here we just outline some of the main differences. In cases of low energy, the values of $S(k_{max})$ are nearly identical for all Lyapunov vectors and there is no special order in $S(k_{max})$ with respect to the index α . The situation is, however, different in the high-energy regime.

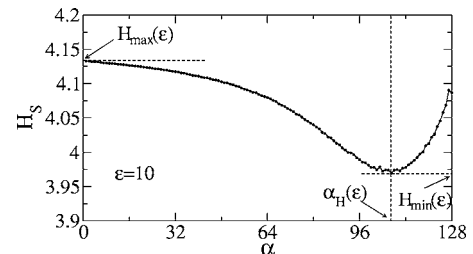


FIG. 10. Spectral entropy $H_S \equiv -\sum S(k) \ln S(k)$ vs α for the FPU- β model with $\epsilon=10$. Note the definitions of the quantities $H_{max}(\epsilon)$, $H_{min}(\epsilon)$, and $\alpha_H(\epsilon)$.

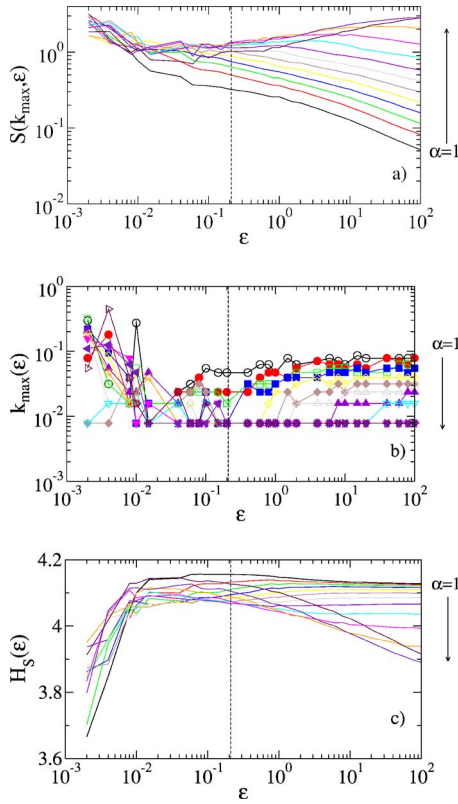


FIG. 11. (Color online) (a) $S(k_{max})$, (b) k_{max} , and (c) H_S against the variation of the energy density ϵ for Lyapunov vectors corresponding to the Lyapunov exponents shown in Fig. 3 for the FPU- β model. The ϵ dependence of all the quantities exhibit smooth transitions in a regime around the critical value $\epsilon_c \approx 0.2$ for the crossover in the Lyapunov spectrum.

With an increase in the energy density, the values of $S(k_{max})$ for the Lyapunov vectors with smaller α decrease gradually, while the values of $S(k_{max})$ for those Lyapunov vectors with larger α increase in the meantime. An ascending order in the values of $S(k_{max})$ with increasing indices α is established gradually along with the growth of the energy density. The crossover between the two kinds of behavior takes place in a regime around the above-mentioned threshold value $\epsilon_c = 0.2$ for the change in the Lyapunov spectrum. The data of k_{max} in the low-energy regime are quite noisy, while some general tendencies of change can be identified from the data in the high-energy regime. For $\epsilon \gg \epsilon_c$, k_{max} of the Lyapunov vectors corresponding to near-zero Lyapunov exponents are close to $2\pi/L$ and the value of k_{max} increases gradually on decreasing the index α from L . Similarly, in cases of low energy density, the dependences of H_S on α have no particular tendency. As the energy density increases beyond a critical value, a descending order in H_S with the growth of α appears gradually. These aspects of the ϵ dependence of the three variables suggest that there are changes in the Lyapunov vectors at the SST and that significant HLMs are only possible in the strong chaotic regime with high energy density. Moreover, the significance of the HLMs increases with the growth of the degree of chaoticity.

To further quantify the significance of HLMs in a case with given energy density, we now define some measures

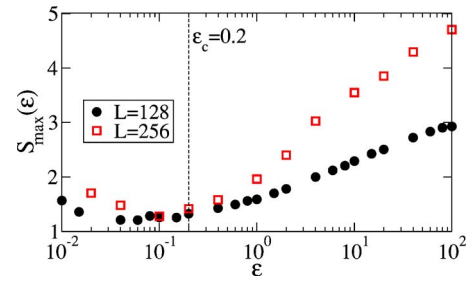


FIG. 12. (Color online) $S_{max}(\epsilon)$ vs ϵ for the FPU- β model. For $\epsilon < \epsilon_c$, the quantity $S_{max}(\epsilon)$ is nearly constant. For $\epsilon > \epsilon_c$, however, $S_{max}(\epsilon)$ increases gradually with ϵ . These facts demonstrate that the significance of hydrodynamic Lyapunov modes grows as the energy density increases. Here, the threshold energy density $\epsilon_c \approx 0.2$ for the transition in the Lyapunov spectrum is shown as a dashed line.

based on the quantities $S(k_{max})$ and H_S , which are already capable of indicating the significance of the possibly wave-like structures in a Lyapunov vector. Two candidates which are suitable for this purpose are the extreme values $S_{max}(\epsilon)$ and $H_{min}(\epsilon)$ (see Figs. 9 and 10 for the definitions). Roughly speaking, $S_{max}(\epsilon)$ represents the height of the highest peak in the static structure factors of all Lyapunov vectors of a case with given ϵ , and H_{min} measures the significance of this peak. We also explore the ϵ dependence of S_{max}/S_{min} and $H_{max} - H_{min}$. These relative measures are expected to be even more suitable for the comparison of cases with different energy densities ϵ .

The variation of $S_{max}(\epsilon)$ with ϵ is plotted in Fig. 12. As can be seen from the figure, $S_{max}(\epsilon)$ is roughly constant as long as the energy density ϵ is lower than the threshold value ϵ_c , although a systematic trend of slow decrease can be recognized for very low energy densities. In contrast, $S_{max}(\epsilon)$ increases gradually with ϵ for $\epsilon > \epsilon_c$. There is also a smooth transition in $H_{min}(\epsilon)$ (see Fig. 13). For $\epsilon < \epsilon_c$, the dependence of $H_{min}(\epsilon)$ on ϵ is rather weak while it decreases gradually with increasing ϵ in the regime $\epsilon > \epsilon_c$. As shown in Fig. 14, the existence of a crossover in the dynamics of the Lyapunov vectors is also reflected in the changes in the ϵ dependences of the relative measures S_{max}/S_{min} and $H_{max} - H_{min}$. Note that the crossover points of these quantities all lie in the regime around the threshold energy density ϵ_c of the transition in the Lyapunov spectrum (see Fig. 2). This implies that both transitions in the Lyapunov spectrum and in the Lyapunov vectors at the SST are possibly manifestations of the same geo-

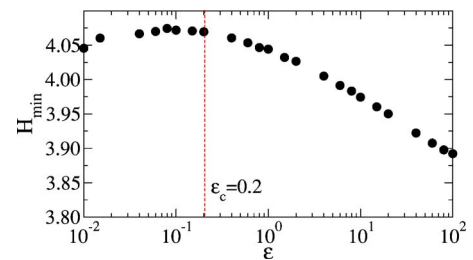


FIG. 13. (Color online) H_{min} vs ϵ for the FPU- β model. The quantity H_{min} is nearly constant for $\epsilon < \epsilon_c$ while it decreases gradually with increasing ϵ for $\epsilon > \epsilon_c$.

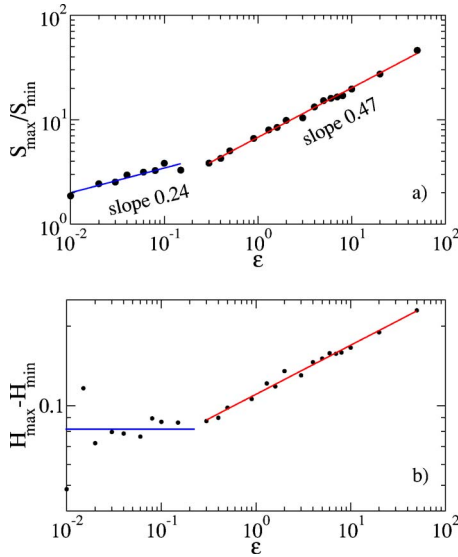


FIG. 14. (Color online) (a) S_{max}/S_{min} and (b) $H_{max}-H_{min}$ vs ϵ for the FPU- β model. In both quantities a change in the ϵ dependence is observed as one crosses the threshold value $\epsilon_c \approx 0.2$.

metric change in the structure of phase space. The variations of these quantities also illustrate that the highest peak in the LV structure factors is more dominant for $\epsilon > \epsilon_c$ than for $\epsilon < \epsilon_c$. Moreover, in the regime beyond the SST, the significance of that peak grows with increasing energy density ϵ .

We present in Fig. 15 the variation of the indices α_S and α_H with ϵ (see Fig. 9 and 10 for the definitions of these indices). The indices normalized by L are rather close to 1.0 in the regime beyond the SST, which means that the corresponding Lyapunov exponents are close to zero. Thus, the associated highest peaks represent certain HLMs. In the regime $\epsilon < \epsilon_c$, however, the normalized indices are relatively far from 1.0, i.e., the corresponding Lyapunov exponents are rather far from zero. This fact, alongside those just mentioned, demonstrates that significant hydrodynamic Lyapunov modes appear only in the regime beyond the SST. Moreover, for $\epsilon > \epsilon_c$, the significance of the HLMs becomes gradually stronger as the energy density increases.

B. FPU- $\alpha\beta$ model

In this subsection, we will show only briefly the changes in the Lyapunov spectrum and the hydrodynamic Lyapunov

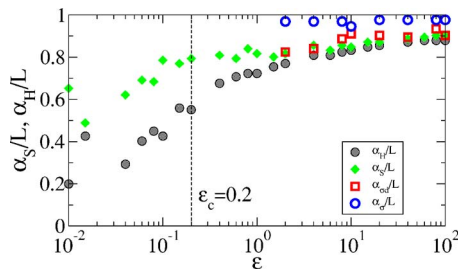


FIG. 15. (Color online) The normalized indices α_S/L and α_H/L are plotted against the energy density ϵ . Note that they are relatively close to 1.0 for $\epsilon > \epsilon_c$. For the purpose of comparison, the quantities $\alpha_{\sigma d}$ and α_{σ} are also presented here. Their definitions are given in Figs. 27 and 28, respectively.

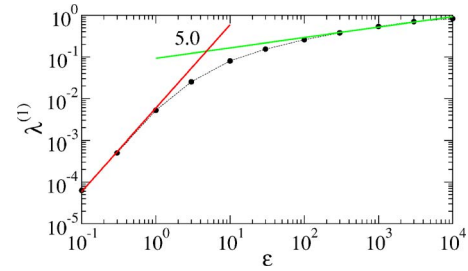


FIG. 16. (Color online) The largest Lyapunov exponent $\lambda^{(1)}$ vs ϵ for the FPU- $\alpha\beta$ model. Similar to the case shown in Fig. 2 for the FPU- β model, there is a crossover in the ϵ dependence of $\lambda^{(1)}$ at $\epsilon_c \approx 5.0$.

modes of the FPU- $\alpha\beta$ model, since the results are qualitatively similar to what we have reported for the FPU- β model.

The variation of the largest Lyapunov exponent $\lambda^{(1)}$ with the energy density ϵ is presented in Fig. 16. As in the case of the FPU- β model, there is a crossover in the ϵ dependence of $\lambda^{(1)}$ and the scaling is different in the regimes beyond and below the threshold value ϵ_c of the crossover [21]. Numerical fitting of the data to a power law $\lambda^{(1)} \sim \epsilon^\beta$ yields $\beta \approx 2.0$ for $\epsilon < \epsilon_c$ and $\beta \approx 0.25$ for $\epsilon > \epsilon_c$, respectively. The threshold energy density of the crossover is estimated as $\epsilon_c \approx 5.0$.

To illustrate further changes in the Lyapunov spectrum, we show in Fig. 17 the ϵ dependences of several Lyapunov exponents sampled from the positive branch of the Lyapunov spectrum. Obviously, their tendency of variation is very similar to that of $\lambda^{(1)}$. The normalized quantities $\lambda^{(\alpha)}(\epsilon)/\lambda^{(\alpha)}(\epsilon_0)$ are plotted in Fig. 18 against the energy density ϵ . As shown in the diagram, all data from different Lyapunov exponents collapse on a single curve, which suggests that all Lyapunov exponents exhibit a crossover at ϵ_c similar to the largest one $\lambda^{(1)}$. This confirms the anticipation that, in connection with the transition from weak to strong chaos, the geometric structure of the phase space changes globally at the SST. Moreover, as in the case of the FPU- β model, the numerical results presented also provide a basis for the quasi-isotropy assumption used in the analytical calculation of the largest Lyapunov exponent [25].

We present in Fig. 19 the normalized quantities $\lambda^{(\alpha)}/\rho_h$, which are assumed to be constant, irrespective of the variation of the energy density, if all the Lyapunov exponents have identical ϵ -dependence. As can be seen from the plot,

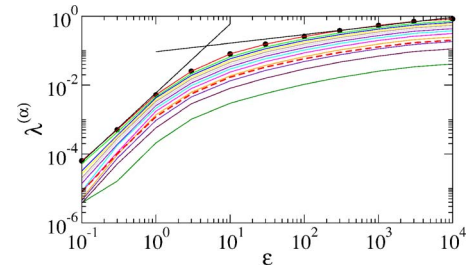


FIG. 17. (Color online) Similar to Fig. 3 but for the FPU- $\alpha\beta$ model. All Lyapunov exponents follow the same tendency of variation as the largest one.

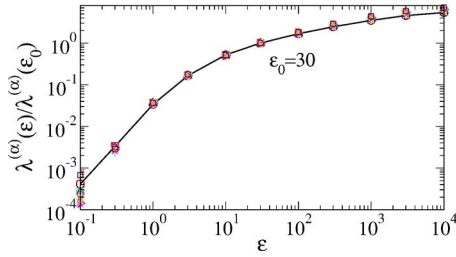


FIG. 18. (Color online) Similar to Fig. 4 but for the FPU- $\alpha\beta$ model. All data from different Lyapunov exponents roughly collapse onto a master curve.

these quantities are nearly constant in the regime of ϵ shown. This fact further demonstrates the correctness of our observation that the tendencies of change of all Lyapunov exponents are almost identical.

The variations of the quantities $S(k_{max})$, k_{max} and H_S for several Lyapunov vectors with the associated Lyapunov exponents in the positive branch of the Lyapunov spectrum are shown in Fig. 20. All three variables exhibit different behavior in the low- and high-energy regimes. Moreover, the crossover in the ϵ dependence of these quantities takes place in a regime around the threshold value $\epsilon_c \approx 5.0$ as in the Lyapunov spectrum of this system (see Fig. 18). The illustrated aspects of the ϵ -dependence of these quantities demonstrate that, alongside the alternations in the Lyapunov spectrum, there are also changes in the Lyapunov vectors at the SST.

The variations of the measures S_{max} and H_{min} with the energy density ϵ are shown in Fig. 21. One can easily see from the plot that both variables display different behaviors in the two regimes divided by the threshold value $\epsilon_c \approx 5.0$. In particular, for $\epsilon > \epsilon_c$, S_{max} ascends gradually with increasing energy density, and H_{min} decreases. In the regime $\epsilon < \epsilon_c$, however, the variable S_{max} increases with decreasing ϵ , and H_{min} decreases in the meantime [49]. From the above discussion one can conclude that the highest peak in the LV structure factors becomes more significant as the energy density departs further from the threshold value ϵ_c .

The normalized indices α_S and α_H presented in Fig. 22 are close to 1.0 for $\epsilon \gg \epsilon_c$, i.e., the corresponding Lyapunov exponents are close to 0. This suggests that in this high-energy regime the highest peak of the LV structure factors represents a certain HLM. In contrast, the indices are close to zero for

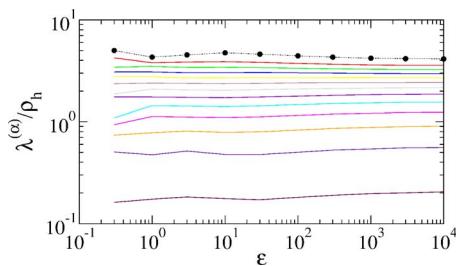


FIG. 19. (Color online) Similar to Fig. 5 but for the FPU- $\alpha\beta$ model. $\lambda^{(\alpha)}/\rho_h$ are nearly constant over the regime of ϵ shown, which indicates that all the Lyapunov vectors have roughly identical tendencies of change with ϵ .

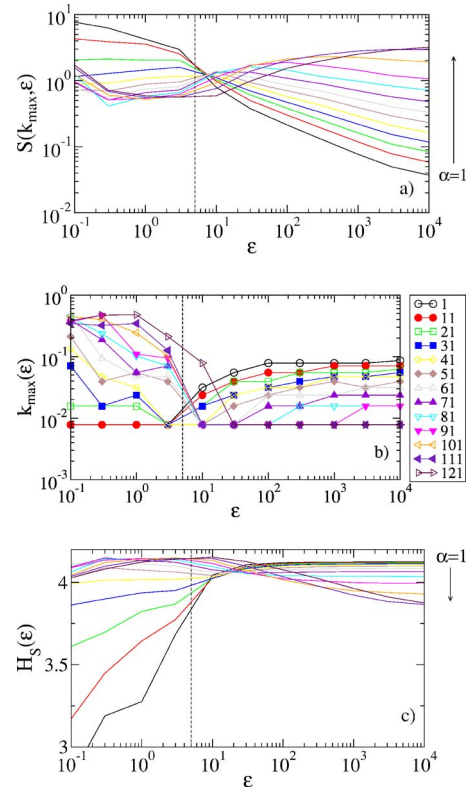


FIG. 20. (Color online) (a) $S(k_{max})$, (b) k_{max} , and (c) H_S against the variation of the energy density ϵ for several Lyapunov vectors corresponding to the Lyapunov exponents shown in Fig. 17. The ϵ dependence of all the quantities exhibits smooth transitions in a regime around the critical value $\epsilon_c \approx 5.0$ of the crossover in the Lyapunov spectrum.

$\epsilon < \epsilon_c$, i.e., the Lyapunov exponents corresponding to the Lyapunov vectors whose static structure factors show the highest peak are far from zero. This demonstrates that the highest peak in the static LV structure factors does not represent a HLM. Therefore, we conclude that the HLMs are more significant in the regime $\epsilon > \epsilon_c$ than in the regime $\epsilon < \epsilon_c$. The increase of S_{max} and the decrease of H_{min} with ϵ in the regime $\epsilon > \epsilon_c$ indicate that HLMs become more significant with increasing ϵ .

Here, we find a scenario of change in the Lyapunov spectrum and the Lyapunov vectors of the FPU- $\alpha\beta$ model which is similar to that in the FPU- β model. This encourages us to surmise that the occurrence of such changes in the Lyapunov characteristics at the SST is typical for a large class of Hamiltonian lattice models.

V. FINITE-SIZE EFFECTS AND THE ROLE OF FLUCTUATIONS IN FINITE-TIME LYAPUNOV EXPONENTS

In the previous sections, we kept the system size $L=128$ to demonstrate the changes of the Lyapunov spectrum and HLMs with varying energy density ϵ . Here, we will see how these results are influenced by the change of the system size L . Since the study of the thermodynamic limit of Lyapunov

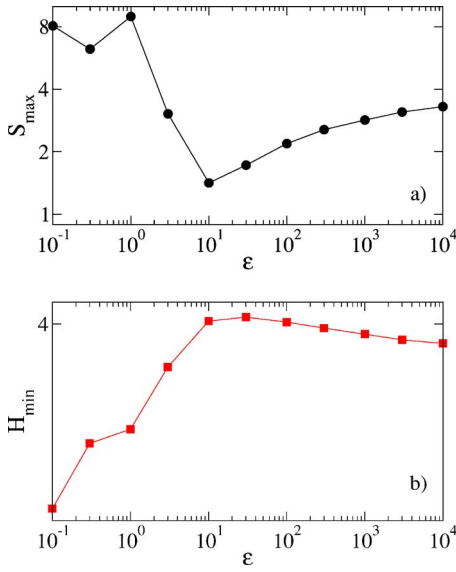


FIG. 21. (Color online) (a) S_{max} and (b) H_{min} vs ϵ for the FPU- $\alpha\beta$ model. Both quantities have different behaviors in the regimes below and beyond the threshold value $\epsilon_c \approx 5$.

characteristics is a substantial topic by itself, we postpone a thorough exploration of related features to a forthcoming publication and show only briefly some essential points in this paper.

It is well known that the Lyapunov spectrum of extended chaotic systems approaches a continuous curve as the system size goes to infinity [50]. The Lyapunov spectra for three cases with different L are shown in Fig. 23 for the FPU- β model. The collapse of data on a single master curve shows that the Lyapunov spectrum with $L=128$, which was used in the previous sections, is already rather close to the limit distribution, and the reported changes of the Lyapunov spectrum at the SST should persist in the thermodynamic limit.

Note that in Fig. 8, for a group of LVs with $\alpha \approx L$, the peak wave-numbers k_{max} take the same value $2\pi/L$. This hinders us from seeing the linear dispersion relation $\lambda \sim k_{max}$ claimed in previous work [37,38]. We will provide numerical evidence for the fact that the apparent condensation of k_{max} at $2\pi/L$ is a finite-size effect. As presented in Fig. 24 for three cases with $L=64$, 128 and 256 respectively, the population of LVs with $k_{max}=2\pi/L$ decreases as the system size increases. It appears that there is a limit curve

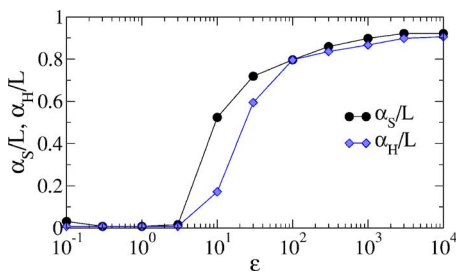


FIG. 22. (Color online) Variation of the indices α_S and α_H with the energy density ϵ . Note that they are close to 1.0 for $\epsilon > \epsilon_c$, which means that the corresponding Lyapunov exponents are close to zero.

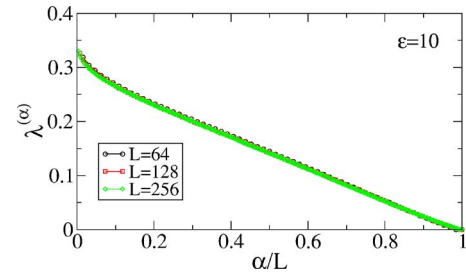


FIG. 23. (Color online) System size dependence of the Lyapunov spectrum of the FPU- β model. The collapse of the data to a single master curve suggests that the finite-size effect on the Lyapunov spectrum can be neglected.

$k(\alpha/L)$ as L goes to infinity, and for a simulation with a finite L , only a part of this asymptotic curve can be recognized from the α dependence of k_{max} due to the finite resolution of k .

Variations of the quantity $S(k_{max})$ with the index α are shown in Fig. 25 for three cases with $L=64$, 128, and 256, respectively. In connection with the change of k_{max} presented in Fig. 24, the increase of the system size L does lead to the increase of $S(k_{max})$ in the regime around S_{max} , i.e., for those LVs whose static LV structure factors have sharp peaks. A comparison of the two figures tells us that the significant changes of $S(k_{max})$ occur in the regime where the value of k_{max} varies with L , i.e., the change in $S(k_{max})$ is mainly due to the improvement of the estimate of the peak position k_{max} . This is consistent with the observation that the change in $S(k_{max})$ is significant for the LVs whose static LV structure factors have sharp peaks.

The ϵ dependence of S_{max} for simulations with $L=256$ was shown in Fig. 12 together with the case $L=128$. As expected, increasing the system size does lead to some changes in the values of S_{max} , especially in the high-energy regime $\epsilon > \epsilon_c$. The discrepancy in the energy density dependence of S_{max} in the low- and high-energy regimes is, however, qualitatively the same for the two cases with different system sizes L . With the variation of the system size L , the changes in the behavior of other quantities characterizing the Lyapunov vectors resemble that of S_{max} . These facts demonstrate that the changes in the Lyapunov vectors at the SST, which were reported in the previous sections, are intrinsic to the treated systems and they will not be changed by a variation in the system size.

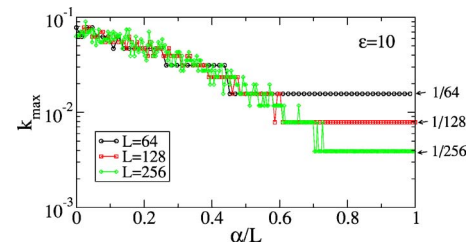


FIG. 24. (Color online) System size dependence of the peak wave number k_{max} of LVs of the FPU- β model. A comparison between data sets with different system sizes L indicates that the apparent condensation of k_{max} at $2\pi/L$ for the LVs with $\alpha \approx L$, which can be observed in Fig. 8, is an effect of a finite system size.

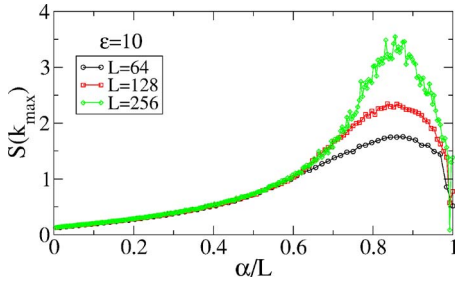


FIG. 25. (Color online) System size dependence of $S(k_{max})$. The significant changes in $S(k_{max})$ occur in the regime where k_{max} changes with the system size L .

Another interesting feature of the L dependence of $S(k_{max})$ is that the value of the normalized index α_S/L is nearly constant, irrespective of the increase in system size (see Fig. 26). Therefore, the deviation of α_S from the intuitive expectation $\alpha_S=L$ is not a finite-size effect and it is necessary to offer an alternative explanation here. We attribute it to the difference in the fluctuations of finite-time Lyapunov exponents.

In previous studies [28] Posch *et al.* have proposed that the different Lyapunov vector dynamics of systems with hard-core or soft-potential interactions is a result of the different nature of the fluctuations of finite-time Lyapunov exponents. The finite-time Lyapunov exponent $\lambda(\tau)$ represents the average instability of trajectory segments of duration τ and it approaches the normal Lyapunov exponent as τ goes to infinity, i.e., $\lim_{\tau \rightarrow +\infty} \lambda(\tau) = \lambda$. The standard deviation $\sigma(\lambda(\tau))$ of $\lambda(\tau)$ is a measure of the fluctuations of finite-time Lyapunov exponents $\lambda(\tau)$, which has been used by Posch *et al.* in previous work to show the difference between systems with hard-core or soft-potential interactions [28]. Here, we prefer to use a relative measure $\sigma(\lambda^{(\alpha)}(\tau))/(\lambda^{(\alpha+1)} - \lambda^{(\alpha)})$, which shows the effective overlap of the distributions of the finite-time Lyapunov exponents with neighboring α . We expect such a quantity to be able to tell us how strong the mixing between the unstable directions represented by Lyapunov vectors is, which controls the significance of HLMs. For instance, a small value of $\sigma(\lambda^{(\alpha)}(\tau))/(\lambda^{(\alpha+1)} - \lambda^{(\alpha)})$ means that the mixing among unstable directions associated with neighboring LVs is relatively weak, i.e., the HLMs are significant.

The variation of $\sigma(\lambda^{(\alpha)}(\tau))/(\lambda^{(\alpha+1)} - \lambda^{(\alpha)})$ with α and the definition of $\alpha_{\sigma d}$ are presented in Fig. 27. The values of $\alpha_{\sigma d}$

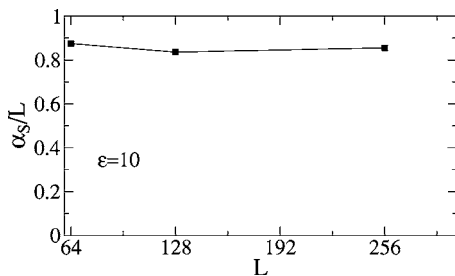


FIG. 26. Numerical simulations show that the value of the normalized index α_S/L (see Fig. 9) is nearly constant, irrespective of the variation in system size L .

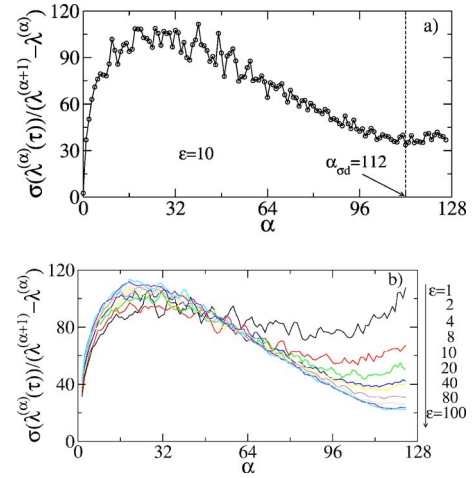


FIG. 27. (Color online) The fluctuations of the finite-time Lyapunov exponents are measured by the quantity $\sigma(\lambda^{(\alpha)} \times (\tau))/(\lambda^{(\alpha+1)} - \lambda^{(\alpha)})$, where $\sigma(\lambda^{(\alpha)}(\tau))$ is the standard deviation of the finite-time Lyapunov exponents with the index α . The quantity $\alpha_{\sigma d}$ is defined as the index corresponding to the minimal value of the quantity $\sigma(\lambda^{(\alpha)}(\tau))/(\lambda^{(\alpha+1)} - \lambda^{(\alpha)})$ in the regime $\lambda^{(\alpha)} \approx 0$.

for several cases with different energy densities ϵ are shown in Fig. 15. They are quite close to the corresponding values of α_S . This confirms our statement that the value of α_S is determined by the nature of the fluctuations of the finite-time Lyapunov exponents. For comparison, the values of α_{σ} , defined with respect to $\sigma(\lambda^{(\alpha)}(\tau))$, are presented in the same figure. The deviation from α_S is rather large compared to the difference between $\alpha_{\sigma d}$ and α_S , which shows the advantage of the relative measure $\sigma(\lambda^{(\alpha)}(\tau))/(\lambda^{(\alpha+1)} - \lambda^{(\alpha)})$ over $\sigma(\lambda^{(\alpha)} \times (\tau))$. The definition of α_{σ} and the variation of $\sigma(\lambda^{(\alpha)}(\tau))$ can be found in Fig. 28.

In addition, Fig. 27 shows that the value of $\sigma(\lambda^{(\alpha)} \times (\tau))/(\lambda^{(\alpha+1)} - \lambda^{(\alpha)})$ in the regime $\alpha \approx L$ decreases gradually as ϵ changes from 1 to 100. This provides an explanation for

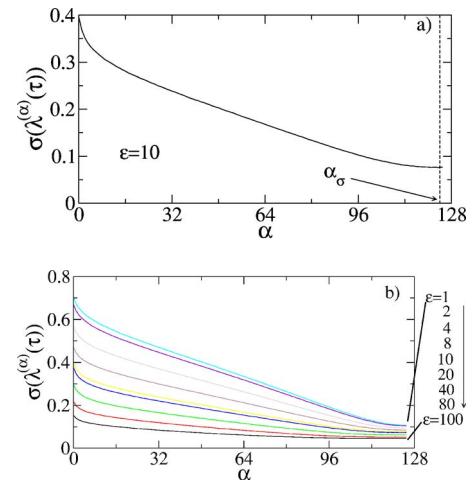


FIG. 28. (Color online) Standard deviation of the finite-time Lyapunov exponents $\sigma(\lambda^{(\alpha)}(\tau))$ vs the index α for (a) $\epsilon=10$ and (b) several cases with different energy densities ϵ . The quantity α_{σ} is defined as the index corresponding to the minimal value of the quantity $\sigma(\lambda^{(\alpha)}(\tau))$ in the regime $\lambda^{(\alpha)} \approx 0$.

the above observation that the significance of the HLMs increases with ϵ in this energy regime (see Figs. 12 and 13). In some respects, the quantity $\sigma(\lambda^{(a)}(\tau))/(\lambda^{(a+1)} - \lambda^{(a)})$ serves as a quantitative measure of the chaoticity of the treated systems. We leave a detailed study of the relation between the fluctuations of finite-time Lyapunov exponents and the significance of HLMs to a future publication.

VI. CONCLUSION AND DISCUSSION

In this study, we have shown that apart from a crossover in the scalings of the energy density dependence of the largest Lyapunov exponent, other Lyapunov exponents of the Hamiltonian lattice models exhibit similar smooth transitions at the SST. The FPU- β model has been selected as an example to illustrate that there exist HLMs in systems of Hamiltonian lattices with continuous symmetries. Some measures have been defined to indicate the significance of HLMs. Numerical simulations demonstrate that these quantities characterizing the significance of HLMs exhibit different behavior in the regimes below and beyond SST. Roughly speaking, significant HLMs are only possible in the regime of strong chaos beyond the SST and there the significance of HLMs grows as the energy density increases. These numerical results give support to the point of view that the transition from weak to strong chaos at the SST manifests a global change in the geometric structure of phase space. Numerical simulations for cases with different system sizes imply that the above-mentioned changes in Lyapunov exponents and vectors at the SST appear to persist in the thermodynamic limit. We discussed briefly the relation between the fluctuations of finite-time Lyapunov exponents and the significance of HLMs.

For the two versions of the FPU model under investigation, all Lyapunov exponents have similar tendencies of change in the regime around the SST. This may have its origin in the nature of the geometric structure of phase space of the two systems. In previous studies Pettini and co-workers found that the sectional curvatures of the manifold representing the dynamics of the two systems are nearly always positive as the energy density increases through the SST [22]. The mechanism of the creation of chaos in these systems is parametric resonance, an instability induced by the oscillation of sectional curvatures instead of the occurrence of negative curvatures. We expect that the scenario of change in the Lyapunov exponents and Lyapunov vectors at the SST as reported in this paper is common for Hamiltonian lattice models where parametric resonance is the only (dominant) origin of chaos. Similar tendencies of change in all Lyapunov exponents may also be the very reason why the analytical method based on the quasi-isotropy assumption is

capable of correctly estimating the largest Lyapunov exponent in certain Hamiltonian lattice models. For the dynamic XY model [19,46–48], in contrast to the FPU model, the occurrence of negative curvatures is another important source of chaos besides parametric resonance. Previous investigations have shown that there are rather large differences between the analytical estimate of the largest Lyapunov exponent based on the quasi-isotropy assumption and the numerical value in the crossover regime where the dominant source of chaos changes from parametric resonance to the occurrence of negative curvatures [25]. Our preliminary simulations show that with varying energy density, the Lyapunov exponents of this system have different tendencies of change except in the low-energy regime close to the harmonic limit. The scenario of change in the Lyapunov vectors is different from, and also quite complex compared to, the cases investigated here. A detailed report on these results for the dynamic XY model is beyond the scope of this work and will be presented elsewhere.

Continuous symmetries and conserved quantities are commonly believed to be essential for the appearance of HLMs. Our investigations in the current paper demonstrate that strong chaos is also important for the appearance of HLMs and the significance of HLMs increases with a growth in the degree of chaoticity. In the low-energy regime below the SST, the dynamics of the systems under investigation is rather close to that of a chain of harmonic oscillators, and all the Lyapunov exponents are nearly degenerate. At least the fluctuations of the finite-time Lyapunov exponents are quite large compared to the differences between the neighboring Lyapunov exponents in the spectrum. These facts prevent a clear decomposition of the tangent space into individual mutually orthogonal subspaces corresponding to the groups of degenerate Lyapunov exponents. In these low-energy cases, there may still be certain long-wavelength structures in the Lyapunov vectors associated with near-zero Lyapunov exponents. These long-wavelength structures are, however, so weak in comparison with those in the cases beyond the SST that we prefer to say that HLMs are only possible in the high-energy regime beyond the SST. Therefore, the SST could be viewed as an effective threshold value for the observation of significant HLMs. Note that, since the explored transitions at the SST are all quite smooth, the threshold values estimated in this paper can only be considered as reference points of qualitative changes while these transitions actually take place in a regime around them.

ACKNOWLEDGMENTS

We acknowledge financial support from the DFG within SFB393 “Parallele Numerische Simulation für Physik und Kontinuumsmechanik.”

- [1] N. S. Krylov, *Works on the Foundations of Statistical Mechanics* (Princeton University Press, Princeton, NJ, 1979).
- [2] P. Gaspard, *Chaos, Scattering, and Statistical Mechanics* (Cambridge University Press, Cambridge, U.K., 1998).
- [3] J. P. Dorfman, *An Introduction to Chaos in Nonequilibrium Statistical Mechanics* (Cambridge University Press, Cambridge, U.K., 1999).
- [4] D. J. Evans, G. P. Morriss, *Statistical Mechanics of Nonequilibrium Liquids* (Academic, New York, 1990).
- [5] W. G. Hoover, *Computational Statistical Mechanics* (Elsevier, New York, 1991).
- [6] W. G. Hoover, *Time Reversibility, Computer Simulation, and Chaos* (World Scientific, Singapore, 1999).
- [7] H. Poincaré, *Les Méthodes Nouvelles de la Mécanique Céleste* (Blanchard, Paris, 1987); E. Fermi, *Nuovo Cimento* **25**, 267 (1923); **26**, 105 (1923).
- [8] E. Fermi, J. Pasta, and S. Ulam (with M. Tsingou), Los Alamos Report No. LA-1940, 1955 (unpublished), in *Collected Papers of Enrico Fermi*, edited by E. Segré (University of Chicago press, Chicago, 1965), Vol. 2, p. 978.
- [9] A. N. Kolmogorov, *Dokl. Akad. Nauk SSSR* **98**, 527 (1954); J. Moser, *Nachr. Akad. Wiss. Goett. II, Math.-Phys. Kl.* **1**, 1 (1962); V. I. Arnold, *Russ. Math. Surveys* **18**, 9 (1963).
- [10] L. Chierchia and G. Gallavotti, *Nuovo Cimento Soc. Ital. Fis.*, B **67**, 277 (1982); G. Benettin, L. Galgani, A. Giorgilli, and J. M. Strelcyn, *ibid.* **79**, 201 (1984); M. Falcioni, U. M. Marconi, and A. Vulpiani, *Phys. Rev. A* **44**, 2263 (1991); N. N. Nekhoroshev, *Funct. Anal. Appl.* **5**, 338 (1971); *Russ. Math. Surveys* **32**, 1 (1977).
- [11] See also L. Galgani, A. Giorgilli, A. Martinoli, and S. Vanzini, *Physica D* **59**, 334 (1992).
- [12] F. M. Izrailev and B. V. Chirikov, *Dokl. Akad. Nauk SSSR* **166**, 57 (1966) [*Sov. Phys. Dokl.* **11**, 30 (1966)].
- [13] P. Bocchieri, A. Scotti, B. Bearzi, and A. Loinger, *Phys. Rev. A* **2**, 2013 (1970).
- [14] R. Livi, M. Pettini, S. Ruffo, M. Sparpaglione, and A. Vulpiani, *Phys. Rev. A* **28**, 3544 (1983); **31**, 1039 (1985); R. Livi, M. Pettini, S. Ruffo, and A. Vulpiani, *ibid.* **31**, 2740 (1985).
- [15] H. Kantz, *Physica D* **39**, 322 (1989).
- [16] M. Pettini and M. Cerruti-Sola, *Phys. Rev. A* **44**, 975 (1991); M. Pettini and M. Landolfi, *ibid.* **41**, 768 (1990).
- [17] See, for example, L. Casetti, M. Cerruti-Sola, M. Pettini, and E. G. D. Cohen, *Phys. Rev. E* **55**, 6566 (1997); D. L. Shepelyansky, *Nonlinearity* **10**, 1331 (1997).
- [18] For a review of the current state, see, for example, M. Pettini, L. Casetti, M. Cerruti-Sola, R. Franzosi, and E. G. D. Cohen, *Chaos* **15**, 015106 (2005).
- [19] D. Escande, H. Kantz, R. Livi, and S. Ruffo, *J. Stat. Phys.* **76**, 605 (1994).
- [20] K. Yoshimura, *Physica D* **104**, 148 (1997).
- [21] M. Cerruti-Sola, M. Pettini, and E. G. D. Cohen, *Phys. Rev. E* **62**, 6078 (2000).
- [22] M. Pettini, *Phys. Rev. E* **47**, 828 (1993).
- [23] L. Casetti and M. Pettini, *Phys. Rev. E* **48**, 4320 (1993).
- [24] L. Casetti, R. Livi, and M. Pettini, *Phys. Rev. Lett.* **74**, 375 (1995).
- [25] L. Casetti, C. Clementi, and M. Pettini, *Phys. Rev. E* **54**, 5969 (1996).
- [26] L. Casetti, M. Pettini, and E. G. D. Cohen, *Phys. Rep.* **337**, 237 (2000).
- [27] H. A. Posch and R. Hirschl, in *Hard Ball Systems and the Lorentz Gas*, edited by D. Szász (Springer, Berlin, 2000), p. 279.
- [28] C. Forster, R. Hirschl, H. A. Posch, and Wm. G. Hoover, *Physica D* **187**, 294 (2004).
- [29] J.-P. Eckmann and O. Gat, *J. Stat. Phys.* **98**, 775 (2000).
- [30] S. McNamara and M. Mareschal, *Phys. Rev. E* **64**, 051103 (2001). M. Mareschal and S. McNamara, *Physica D* **187**, 311 (2004).
- [31] A. S. de Wijn and H. van Beijeren, *Phys. Rev. E* **70**, 016207 (2004).
- [32] T. Taniguchi and G. P. Morriss, *Phys. Rev. E* **65**, 056202 (2002); **68**, 026218 (2003); *Phys. Rev. Lett.* **94**, 154101 (2005).
- [33] J.-P. Eckmann, C. Forster, H. A. Posch, and E. Zabey, *J. Stat. Phys.* **118**, 813 (2005).
- [34] H. L. Yang and G. Radons, *Phys. Rev. E* **71**, 036211 (2005).
- [35] G. Radons and H. L. Yang, e-print nlin.CD/0404028.
- [36] C. Forster and H. A. Posch, *New J. Phys.* **7**, 32 (2005).
- [37] H. L. Yang and G. Radons, *Phys. Rev. E* **73**, 016202 (2006); **73**, 016208 (2006).
- [38] H. L. Yang and G. Radons, *Phys. Rev. Lett.* **96**, 074101 (2006).
- [39] The standard RK4 algorithm is used for most results reported here. For the integration step sizes used, the Hamiltonian structure of the system dynamics is reasonably well preserved during our simulations. This fact is partially evident from the symmetry of the Lyapunov spectrum (see, e.g., Fig. 1). The simulations for the case of the FPU- β model have been checked with the symplectic version of RK4 proposed by J. M. Sanz-serva and M. P. Calvo, *Numerical Hamiltonian Problems* (Chapman and Hall, London, 1994).
- [40] G. Benettin, L. Galgani, and J. M. Strelcyn, *Phys. Rev. A* **14**, 2338 (1976); G. Benettin, L. Galgani, A. Giorgilli, and J. M. Strelcyn, *Meccanica* **15**, 9 (1980); **15**, 21 (1980); I. Shimada and T. Nagashima, *Prog. Theor. Phys.* **61**, 1605 (1979).
- [41] H. Chaté, *Europhys. Lett.* **21**, 419 (1993).
- [42] J. P. Boon and S. Yip, *Molecular Hydrodynamics* (McGraw-Hill, New York, 1980).
- [43] Y. Pomeau, A. Pumir, and P. Pelce, *J. Stat. Phys.* **37**, 39 (1984); K. Kaneko, *Physica D* **23**, 436 (1986).
- [44] For the study of the localization of Lyapunov vectors in molecular systems, see Lj. Milanovic and H. A. Posch, *J. Mol. Liq.* **96-97**, 221 (2002).
- [45] A. Pikovsky and A. Politi, *Nonlinearity* **11**, 1049 (1998); *Phys. Rev. E* **63**, 036207 (2001).
- [46] P. Butera and G. Caravati, *Phys. Rev. A* **36**, 962 (1987).
- [47] C. Giardiná, R. Livi, A. Politi, and M. Vassalli, *Phys. Rev. Lett.* **84**, 2144 (2000).
- [48] O. V. Gendelman and A. V. Savin, *Phys. Rev. Lett.* **84**, 2381 (2000); A. V. Savin and O. V. Gendelman, *Phys. Solid State* **43**, 355 (2001).
- [49] Note that in the low-energy regime of the FPU- $\alpha\beta$ model the behavior of S_{max} and H_{min} is different from the FPU- β model (compare Fig. 21 with Figs. 12 and 13]). We attribute this to peaks in the spectrum $S(k)$ at large k values not related to hydrodynamic Lyapunov modes (see Fig. 22). Probably this is related to differences in the integrable structures in both models.
- [50] See, for example, Livi *et al.*, *J. Phys. A* **19**, 2033 (1986).